Marine Chemistry xxx (xxxx) xxx–xxx

Contents lists available at ScienceDirect

Marine Chemistry

journal homepage: www.elsevier.com/locate/marchem

Quantitative interpretation of vertical profiles of calcium and pH in the coral coelenteron

Xiangcheng Yuan[a], Wei-Jun Cai[b,*], Christof Meile[c], Brian M. Hopkinson[c], Qian Ding[d], Verena Schoepf[e,f], Mark E. Warner[b], Kenneth D. Hoadley[b], Bingzhang Chen[g], Sheng Liu[a], Hui Huang[a], Ying Ye[d], Andréa G. Grottoli[e]

[a] Key Laboratory of Marine Bio-resources Sustainable Utilization and Guangdong Provincial Key Laboratory of Applied Marine Biology, South China Sea Institute of Oceanology, Chinese Academy of Sciences, Guangzhou 510000, China
[b] School of Marine Science and Policy, University of Delaware, Newark, DE 19716, USA
[c] Department of Marine Sciences, The University of Georgia, GA 30602, USA
[d] Ocean College, Zhejiang University, Hangzhou 310058, China
[e] School of Earth Sciences, The Ohio State University, Columbus, OH, USA
[f] ARC Centre of Excellence for Coral Reef Studies, School of Earth Sciences and UWA Oceans Institute, The University of Western Australia, Crawley, WA, Australia
[g] Ecosystem Dynamics Research Group, Research and Development Center for Global Change, Japan Agency for Marine-Earth Science and Technology, Yokohama, Japan

ARTICLE INFO

Keywords:
Microsensors
Coral coelenteron
Ocean acidification
Calcification

ABSTRACT

Scleratinian corals (hard corals) and their symbiotic algae are the ecological engineers of biodiverse and geological important coral reef habitats. The complex, linked physiological processes that enable the holobiont (coral + algae) to calcify and generate reef structures are consequently of great interest. However, the mechanism of calcification is difficult to study for several reasons including the small spatial scales of the processes and the close coupling between the symbiont and host. In this study, we explore the utility of pH and Ca^{2+} microelectrodes for constraining the rates and spatial distribution of photosynthesis, respiration, and calcification. The work focuses on vertical profiles of pH and Ca^{2+} through the coelenteron cavity, a semi-isolated compartment of modified seawater amenable to quantitative interpretation. In two studied species, *Turbinaria reniformis* and *Acropora millepora*, Ca^{2+} concentrations decreased in a roughly linear manner from the mouth to the base of the coelenteron, indicating the primary physiological process affecting Ca^{2+} concentration is removal for calcification below the coelenteron. In contrast, the H^+ concentration remained relatively constant over much of the coelenteron cavity before it increased sharply toward the base of the coelenteron, indicative of proton-pumping from the calcification fluid below. The estimated H^+ gradient between the coelenteron cavity and the calcification site was > 10 times higher than previously predicted. Consequently, the energy required to export protons from the calcifying fluid was estimated to be ~3 times higher than previously calculated. A one-dimensional reaction-diffusion model was used to interpret the pH profile considering the effects of photosynthesis, respiration, and calcification. This model provided a good fit to the observed pH profile and helped to constrain the rates and spatial distribution of these processes. Our modeling results also suggested that adult corals with deeper polyps may be more sensitive to ocean acidification (OA) because of enhanced difficulty to transport H^+ out of the coelenteron and into the surrounding seawater.

1. Introduction

Corals have chemically distinct micro-environments both within and surrounding the polyps (Agostini et al., 2011; Al-Horani et al., 2003) compared to the surrounding seawater. These semi-isolated environments include the diffusive boundary layer (DBL) on the surface of the coral, the coelenteron (Al-Horani et al., 2003; de Beer et al., 2000), and the calcifying fluid (Anagnostou et al., 2012; McCulloch et al., 2012; Ries, 2011a). By studying biochemical processes in these coral micro-environments, in addition to more common large-scale studies of coral reef ecosystems (DeCarlo et al., 2017), one may understand better how corals transport CO_2 and possibly HCO_3^- from seawater to the interior to support calcification (Cai et al., 2016), and how waste (e.g., proton or H^+) is removed from the interior. This knowledge can then be used to gain insight necessary for predicting how corals will respond to future climate and environmental stresses such as ocean acidification

* Corresponding author.
E-mail address: wcai@udel.edu (W.-J. Cai).

https://doi.org/10.1016/j.marchem.2018.06.001
Received 23 April 2018; Received in revised form 16 June 2018; Accepted 17 June 2018
0304-4203/ Published by Elsevier B.V.

(OA) (Agostini et al., 2011; Ries, 2011b).

The need to better understand the response of corals to global change variables including OA and rising temperature has driven a renewed interest in coral physiology. While calcification rates of corals are typically reduced at elevated pCO_2, in some cases rates are not severely affected or are even stimulated (Huang et al., 2014; Ries et al., 2010; Schoepf et al., 2013). Clearly, the mechanistic details behind the effects of OA on calcification are complex, and multiple explanations have been put forward (Ries, 2011b). A better understanding of the mechanisms by which OA alters calcification rates will help improve predictions about the future fate of marine ecosystems such as coral reefs.

One possible mechanism by which OA may reduce calcification rates is increased diffusive influx of CO_2 into the calcifying fluid due to increasing CO_2 concentrations in seawater, which causes a reduction in the pH and aragonite saturation state of the calcifying fluid (Comeau et al., 2017). On the other hand, one may argue that increased CO_2 transport may benefit calcification, as it supplies inorganic carbon to the high pH and low CO_2 environment of the calcifying fluid (Allison et al., 2014; Cai et al., 2016). These competing possible outcomes highlight the need for a greater understanding of coral physiology and the response of corals to global change.

Recent advances in coral biochemistry have come from a variety of different approaches, including molecular (Drake et al., 2018; Mass et al., 2013), geochemical (Allison et al., 2014; Comeau et al., 2017), and mineralogical perspectives (Falini et al., 2015). In this study, we used microsensors to investigate the coral gastrovascular cavity portion of the coelenteron, which is above the gastrodermis, mesoglea and calicodermis (Fig. 1A). Two tissue layers surround the sac-like coelenteron cavity, and all polyps in a colony are connected through the coenosarc (Fig. 1A) (Agostini et al., 2011). The fluid inside the coelenteron can be shared among the polyps through the coenosarc and can be exchanged with the surrounding water through the mouth (Agostini et al., 2008). The gastrovascular cavity portion of the coelenteron is a semi-isolated compartment containing fluid that originates from seawater and then is modified by metabolic processes. Because the chemistry of seawater is very well understood and since there is presumably no direct homeostatic maintenance of ion concentrations in the coelenteron, this compartment is potentially an interpretable integrator of metabolic processes in the surrounding tissues. Renewal rates of the coelentric fluid are slow (Agostini et al., 2011), making the system accessible to relatively simple numerical models. Thus, the gastrovascular cavity fluid chemistry will be affected by photosynthesis, respiration, and calcification as inorganic carbon, Ca^{2+}, and protons necessary for these processes pass through this compartment.

Compared to the pH in coral coelenterons, recent studies have focused more on the pH of the calcifying fluid. For example, boron isotope studies suggest that pH in the calcifying fluid ranges from 8.4 to 8.7 at a typical seawater pH of ~8.1 (Anagnostou et al., 2012; McCulloch et al., 2012). Complimentary studies using microelectrodes and pH-sensitive dyes indicate that calcifying fluid pH can be elevated by 0.6–2 units above seawater during the daytime (Al-Horani et al., 2003; Cai et al., 2016; Holcomb et al., 2014; Ries, 2011b; Venn et al., 2011; Venn et al., 2009). However, less attention has been paid to how CO_2 and H^+ behave in the coelenteron before CO_2 enters (or H^+ leaves) the calcifying fluid, and how ions and molecules are exchanged between the coelenteron and the calcifying fluid. In addition, previous studies have only investigated the H^+ and Ca^{2+} concentrations at one specific point within the coelenteron (Al-Horani et al., 2003), thus limiting our understanding how coral internal chemical processes and the diffusive exchange with external seawater can influence the coral calcifying fluid.

To study the ion transport processes between different coral compartments (seawater, coelenteron, and calcifying fluid), a calcification model at the coral polyp scale has been recently developed (Hohn and Merico, 2012; Nakamura et al., 2013). This model presents a detailed description of the CO_2 system in the different compartments of a coral and the coral responses to ocean acidification (Hohn and Merico, 2012). Furthermore, Nakamura et al. (2013) developed a coral photosynthesis and calcification model, which reconstructed "light-enhanced calcification" and incorporated respiration rate variation under light and dark conditions. These box-model studies focused on the ion exchanges between different coral compartments, but the molecular and ionic diffusive processes and detailed information on processes within the coelenteron, in particular the depth profiles, were ignored. To bridge this knowledge gap, we collected high resolution vertical profiles of the chemical species H^+ and Ca^{2+} through the coelenteron as a way to assess the metabolic processes that occur within the coral polyp. Both H^+ and Ca^{2+} are relevant to calcification, and H^+ is also altered by photosynthesis and respiration. The reef corals *Turbinaria reniformis* and *Acropora millepora* were selected 1) to examine high resolution vertical gradients of pH and Ca^{2+} in the coelenterons and 2) to interpret these profiles using a reaction-diffusion model. This is the first time that a spatially resolved (in the vertical direction) coupled diffusion-reaction model has been used to study all CO_2 species and the H^+ species in a coral polyp.

2. Methods

2.1. Preparation of coral samples

Small fragments of *Acropora millepora* ($n = 3$) and *Turbinaria reniformis* (n = 3) were taken from the same parent colonies as in a companion study (Schoepf et al., 2013), which were originally collected

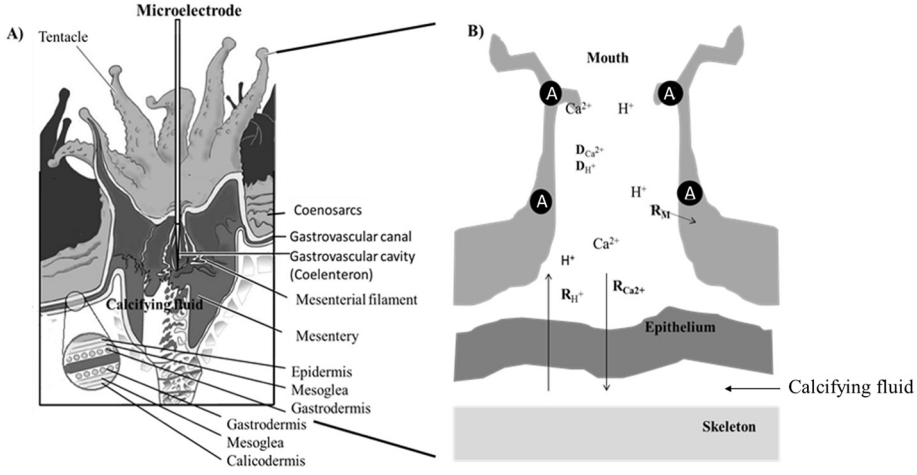

Fig. 1. A) Cross-section of coral polyp with an inserted microelectrode (adapted from Galloway et al. 2006). B) Reactions occur in the gastrovascular cavity (i.e. coelenteron) as follows: 1) Ca^{2+} and H^+ ($cm^{-2}\,s^{-1}$) (D_{Ca} and D_{H^+}) diffuse into the coelenteron via the mouth, 2) H^+ is exchanged with coral host tissue via coral metabolic processes of photosynthesis and respiration (R_M), and 3) Ca^{2+} (R_{Ca}) and H^+ (R_{H+}) are exchanged through the calicodermis as part of calcification. A = endosymbiotic algae.

in northwest Fiji. All coral fragments were shipped to the University of Georgia in April 2012, and were acclimated to a closed-system laboratory aquarium for at least two weeks prior to conducting microelectrode profile measurements in the laboratory. Coral fragments were maintained in a recirculating 100 L aquarium with commercially available artificial seawater (Instant Ocean Reef Crystals) at 26 ± 0.1 °C with a salinity of 32.0 ± 0.1‰, alkalinity of 1800 to 2100 μmol/kg, and a pH_{NBS} of 8.1 to 8.3. A All corals were cultured under a light-dark cycle of 12:12 h for ~4–8 weeks, and the light density is ~200 μmol quanta $m^{-2} s^{-1}$ (Deep Blue Professional, Ltd).

pH and temperature were monitored daily (see below). Polyps from each fragment of each species were microprofiled in June to August 2012. All pH electrodes were recalibrated daily to NBS standards and independent measurements of pH and alkalinity were made using an AS-ALK2 (Apollo SciTech Inc) titrator according to published protocols (Cai et al., 2010).

2.2. Seawater alkalinity and pH

Total alkalinity of seawater was measured using Gran titration methods calibrated with certified reference material from A. Dickson of the Scripps Institute of Oceanography (La Jolla, USA) before each microelectrode measurement profile. Seawater pH was monitored with an Orion Ross pH glass electrode calibrated with NBS pH buffers every day. Total DIC, $[CO_3^{2-}]$, $[HCO_3^-]$, dissolved CO_2 ($[CO_2]_{aq}$), and pCO_2 of the gas in equilibrium with the experimental seawater were calculated from measured values of temperature, salinity, total alkalinity, and pH using the program CO2SYS with Roy et al. (1993) values for the carbonic acid constants.

2.3. Construction of pH and Ca^{2+} microelectrodes

pH and Ca^{2+} were separately measured with liquid membrane pH and Ca^{2+} microelectrodes, with a tip diameter between 10 and 15 μm. Procedures for making, calibrating, and evaluating the stability of these electrodes (Table 1) have been reported previously (Ammann, 1986; Cai et al., 2000; de Beer et al., 2000; Han et al., 2014; Zhao and Cai, 1999). The pH electrodes were calibrated in standard pH buffer 7, 9 and 10 (NBS scale, Thermo Scientific). Ca^{2+} microelectrodes were calibrated with calcium standard solutions (5, 10, and 20 mmol L^{-1}) (de Beer et al., 2000; Han et al., 2014). To prepare these standard solutions, a known amount of $CaCO_3$ powder was added to HCl and diluted with artificial, calcium-free seawater. Different concentrations were made by serial dilution.

2.4. Measurement of pH and Ca^{2+} in coral coelenterons

Prior to each microprofile measurement, a coral fragment was selected and transferred to the microprofiling setup and allowed to acclimate for ~30 min. The microprofiling setup is similar to what was described in Cai et al. (2016). In brief, the microprofiling setup consisted of a beaker containing seawater that was partially immersed in a thermostated water bath (Fisher Scientific), which maintained a constant temperature of 26 °C. The coral was placed on a porous platform within the beaker where the circulation rate was maintained by a stir bar below the platform. However, there was no flow in the intra-polyp environment during the profile data acquisition period. The microelectrodes were connected to a pH meter (Thermo Scientific) with a Ross reference electrode (Thermo Scientific). A commercial combination glass electrode (Orion Ross) monitored the pH of the seawater in the beaker containing the coral. pH microelectrodes were calibrated on the NBS scale, which is about 0.1–0.15 unit greater than that on the total proton scale.

All microsensors were positioned above a selected coral polyp by a motorized micromanipulator using a Kloehn digital syringe pump (Kloehn Co. LTD) fixed on a 2-D micromanipulator base. The vertical advancement was controlled by a computer and custom-made software. The software controlled the microelectrodes to advance through coral polyps at 50 μm increments. In all coral samples, measurements were done with the microelectrode, and the vertical side of the polyps selected for measurements was parallel to the microelectrodes. The coral tissue contracted when the tip initially penetrated into the mouth allowing the point at which the microelectrode entered the coral mouth to be precisely determined. All depths are relative to the coral mouth (depth = 0), where positive depths indicate positions within the coelenteron and negative values indicate positions outside of the coral's mouth. The electrode was then advanced through the polyp's gastrovascular cavity until the microelectrode broke on the skeleton (see details in (Cai et al., 2016)).

The pH reading was considered stable when drift was < 0.2 mV or 0.003 pH units min^{-1} or a total of 3 min had passed, whichever was first. A 3-min limit was established because our pH microelectrodes had a much shorter response time (Zhao and Cai, 1999), but, in some cases, a stable reading was not realistic due to polyp movement. The pH error was ± 0.04 unit in the coelenteron (Cai et al., 2016). Newly produced electrodes show near Nerstian behavior. The signal drift was less than ~0.5–0.6 mV h^{-1}.

Table 1
Performances of the three microelectrodes.

Microelectrode	Response range	Slope (mV $unit^{-1}$)	Lifetime (days)	Drift (mV h^{-1})
pH	5.5–12	58 ± 2	14	0.5
Ca^{2+}	5–30 mM	29 ± 1	7	0.6

2.5. Model description

To help interpret the concentration profiles, a numerical model was developed for the coelenteron that considers diffusive transport, acid-base reactions involving dissolved inorganic carbon (DIC), coral photosynthesis and respiration, and calcification. The composition of the external seawater was set as a fixed concentration starting at a depth of zero. While calcification occurs in the calcifying fluid below the coelenteron, in our model, calcification is set to take place in the layer at the bottom of the profile (Fig. 1B).

The concentration profile of Ca^{2+} is thus described by:

$$\frac{\partial[C_a{}^{2+}]}{\partial t} = D_{C_a{}^{2+}}\frac{\partial^2[C_a{}^{2+}]}{\partial x^2} - R_{C_a} \quad (1)$$

where D_{Ca} is the diffusion coefficient of Ca^{2+} in seawater (Katz and Ben-Yaakov, 1980; Li and Gregory, 1974), and x is coelenteron depth. The rate of calcification (R_{Ca}) is 0 throughout the profile in the coelenteron and only active in the calcifying fluid represented by the bottom layer.

The concentrations of H^+ and DIC species are also affected by coral metabolism (i.e., photosynthesis and respiration) and by acid-base equilibrium reactions (i.e., $H_2O + CO_2 \leftrightarrow H^+ + HCO_3^-$ and $HCO_3^- \leftrightarrow H^+ + CO_3^{2-}$). Thus, for H^+ we have,

$$\frac{\partial[H^+]}{\partial t} = D_{H^+}\frac{\partial^2[H^+]}{\partial x^2} + R(H^+) - R_M \times \frac{17}{106} + 2R_{C_a} \quad (2)$$

where D_{H^+} is the diffusion coefficient of H^+ (Li and Gregory, 1974); $R(H^+)$ is the net rate of proton production or consumption driven by the carbonate acid-base equilibrium; R_M is the metabolism (or net CO_2 production rate), reflecting gross photosynthesis minus respiration; and 17/106 is the Redfield ratio between proton production (or alkalinity consumption) and CO_2 production (Cai et al., 2010). The Ca^{2+} import to the site of calcification at the bottom of the coelenteron must be balanced by the export of an equivalent charge, presumably protons, irrespective of the specific pathway. Thus, at the base of the

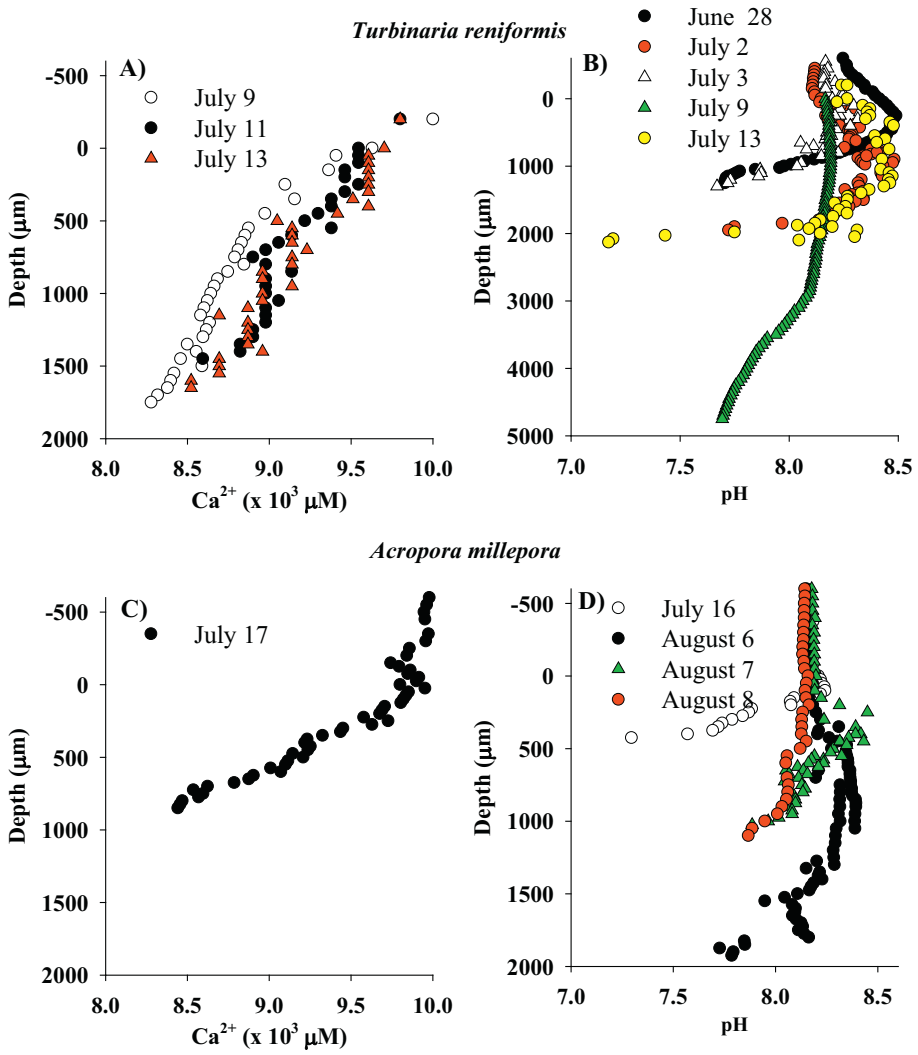

Fig. 2. Vertical profiles of Ca^{2+} and pH_{NBS} through the coelenteron of polyps of *Turbinaria reniformis* (A, B) and *Acropora millepora* (C, D). Polyps of the same colony of each species were measured in June and July 2012. Polyps from two additional colonies of each species were measured in August 2012 at the University of Georgia. Measurements were not repeated in the same polyps. Note: the y scale in panel B is different from the others.

coelenteron, calcification leads to the addition of protons at a rate of $2 \times R_{Ca}$ (Ries, 2011b). With no calcification activity inside the coelenteron, we assume that CO_2 can freely diffuse from the coelenteron into the calcifying fluid (Sültemeyer and Rinast, 1996), providing the DIC to sustain calcification. Thus, the R_{Ca} term only appears in the CO_2 equation but not in the CO_3^{2-} equation, and the governing equations for the DIC species are:

$$\frac{\partial[CO_2]}{\partial t} = D_{CO_2}\frac{\partial^2[CO_2]}{\partial x^2} + R(CO_2) - R_M - R_{Ca} \quad (3)$$

$$\frac{\partial[HCO_3^-]}{\partial t} = D_{HCO_3^-}\frac{\partial^2[HCO_3^-]}{\partial x^2} + R(HCO_3^-) \quad (4)$$

$$\frac{\partial[CO_3^{2-}]}{\partial t} = D_{CO_3^{2-}}\frac{\partial^2[CO_3^{2-}]}{\partial x^2} + R(CO_3^{2-}) \quad (5)$$

where D(i) are the diffusion coefficients of CO_2, HCO_3^-, and CO_3^{2-} (Li and Gregory, 1974), respectively; R(i) are the net carbonate acid-base reaction rates, computed based on the parameterization given in (Zeebe and Wolf-Gladrow, 2001). When the CO_2 flux was assumed to be the main source of DIC to photosynthesis (e.g. net photosynthetic rates, R_M) and calcification (R_{Ca}), the simulation of H^+ could be perfectly fitted to measured data. Hence, R_{Ca} is not present in eqs. 4 and 5, which is consistent with previous evidence showing that CO_2 is an essential source of DIC for coral and CO_3^{2-} cannot be transported into the calcifying fluid (Allison et al., 2014; Cai et al., 2016; Cohen and McConnaughey, 2003; Furla et al., 2000).

The volumetric calcification rate is estimated from the Ca^{2+} profiles, by dividing the flux calculated from the observed (linear) Ca^{2+} concentration gradient in the coelenteron by the thickness of the model calcifying layer. For the model, we limited coral net photosynthesis to daytime and assumed a constant rate with depth in the polyp. R_M was initialized to a value of $\sim 2\,\mu mol\,L^{-1}\,s^{-1}\,cm^{-2}$ based on net photosynthetic rates reported for the parent colonies by (Hoadley et al., 2015). Simulations were started with seawater conditions and run to steady state.

Atmospheric CO_2 partial pressure (pCO_2) is expected to double by the end of this century causing a drop in seawater pH_{NBS} to ~7.8 (Orr et al., 2005). Hence, we chose pH_{NBS} of 7.8 to represent the end of this century conditions in our model and a pH_{NBS} of 8.2 to represent current seawater pH. To isolate the effect of seawater pH on the models, metabolic and calcification rates were also assumed to be constant to investigate the carbonic ion diffusion in response to OA. In addition, the temperature was maintained at 26 or 30 °C and the dissolved inorganic carbon concentration in seawater was set to 1.95 mM in our modeling.

The energy (Nernst potential) required to maintain a H^+-gradient is the minimum energy required to maintain an H^+-gradient across the

cell membranes (i.e. two cell layers (aboral endoderm and calicoderm) and mesoglea, which separates the calcifying fluid from the coelenteron. This energetic requirement can be expressed by the Nernst equation (Ries, 2011b):

$$E = \frac{RT}{nF} \times ln\left(\frac{[H^+]_E}{[H^+]_I}\right) \quad (6)$$

where n is the valence charge of H^+ (which is 1), F is the Faraday constant (96,485.3C mol^{-1}), R is the universal gas constant (8.31451 $J\,K^{-1}\,mol^{-1}$), T is absolute temperature (298.16 at 25 °C), and $[H^+]_E$ and $[H^+]_I$ are H^+ concentrations of the external seawater and of the organism's calcifying fluid, respectively.

2.6. Statistical analysis

The stability of the microelectrode was tested by repeated pH microelectrode profile readings inside a *T. reniformis* coral polyp (data shown in (Cai et al., 2016)). Data were tested for homogeneity of variance and normality of residuals. Statistical analyses (ANOVA) were performed for a significance level of 0.05 using the aov function in R (Version 3.1.1).

3. Results

3.1. Vertical profiles of Ca^{2+} and H^+

The coelenteron depth was 1200 to almost 5000 µm in *Turbinaria reniformis* and, ~500 to 2000 µm in *Acropora millepora* (Fig. 2). Ca^{2+} decreased approximately linearly from the coral mouth to the base of the coelenteron in both species (Fig. 2A and C). The slope values for the calcium decrease were 0.6 ± 0.06 µM µm^{-1} in *T. reniformis* and 1.9 µM µm^{-1} in *A. millepora*. Based on the Ca^{2+} profile, the Ca^{2+} flux was about $5 \pm 0.5 \times 10^{-5}$ µmol cm^{-2} s^{-1} (ca. 0.43 ± 0.04 mg $CaCO_3$ cm^{-2} d^{-1}) in *T. reniformis*, and 16×10^{-5} µmol cm^{-2} s^{-1} (ca. 1.36 mg $CaCO_3$ cm^{-2} d^{-1}) in *A. millepora* (Table 2). The calcium profiles decreased progressively with depth, indicating the main calcium removal site was at the base of the coral, and did not occur within the coelenteron.

In both species, pH was relatively constant as the microelectrode first entered the polyp mouth, then increased by a few tenths of a pH unit in the upper part of the coelenteron before decreasing to ~7.0–7.8 at the base of the coelenteron when outside seawater pH was ~8.1–8.2 (Fig. 2B and D). In *T. reniformis*, pH increased slightly from bulk seawater to a maximum value of 8.5 near the coral surface. However, in *A. millepora*, pH was relatively constant through the diffusive boundary layer (DBL). In contrast to the relatively constant Ca^{2+} profiles, pH profiles substantially varied between measurements in different polyps.

3.2. Carbonate system profiles at different seawater pH and temperature conditions

Using the numerical reaction-diffusion model described in the Methods, we estimated coelenteron CO_2, bicarbonate, carbonate, DIC and total alkalinity (TA) under different seawater pH and temperature conditions (Fig. 3). The model outputs showed that when seawater pH_{NBS} decreases from 8.2 to 7.8, it results in a 4-fold increase in CO_2 concentration, a > 10-fold increase in H^+ concentration, a ~100 µM decrease in carbonate, a ~200 µM increase in DIC, and no real change in TA near the base of the coral coelenteron (Fig. 3). In addition, the temperature variations had very minor effects on all of the modeled profiles compared to variations in external pH (Fig. 3).

Table 2
Coelenteron depth (mm), Ca^{2+} exchange rates and buoyant weight based calcification rate. $R_{Ca}{}^a$ and $R_{Ca}{}^b$ are Ca^{2+} exchange rates using units of µmol cm^{-2} s^{-1} and mg cm^{-2} d^{-1}, respectively, at the bottom of the coelenteron. Cal^c (mg cm^{-2} d^{-1}) is the buoyant weight based calcification rate from Schoepf et al. (2013) under ambient control conditions (i.e., temperature 26.5 °C and pH 8.07). Ca^{2+} profile was only measured once in *A. millepora*.

	Coelenteron depth	$R_{Ca}{}^a$	$R_{Ca}{}^b$	Cal^c
T. reniformis	~1–5	$5 \pm 0.5 \times 10^{-5}$ (n = 3)	0.43 ± 0.04	0.24
A. millepora	~0.5–2	16×10^{-5} (n = 1)	1.36	0.07

4. Discussion

4.1. Technical advantages and limitations

Microelectrodes are a powerful tool for the direct measurement of chemical concentrations within organisms. The reliability and accuracy of pH and other concentration measurements in corals using microelectrodes have previously been established (Cai et al., 2016). Microelectrodes have the unparalleled advantage in measuring fine scale, in situ carbonate chemistry inside a coral polyp rapidly and with minimal disturbance to the organism (Cai et al., 2016). Our tests show that duplicated profiling inside the coelenteron can generate consistent results when the advancement of the electrode is carefully controlled. However, microelectrodes are fragile and inevitably break when they contact with the coral hard skeleton, making repeat profiles impossible. In addition, a polyp may move or release chemicals if it is touched by the microelectrode tip, which could lead to a change in the microenvironment. Thus, we chose to measure each profile with a new microelectrode in a new polyp except during sensor stability tests. Therefore, profiles are effectively independent from each other. Replicate measurements had to be conducted in polyps, which may have differed in depth and/or metabolic activity and may have been measured on different dates. While this resulted in some relative variability in H^+ profiles, the dataset was well suited for the development of numerical models that integrated the observations and provided a mechanism to investigate the effect of changes in ocean water composition on coelenteron biochemistry.

4.2. The implications of Ca^{2+} profiles

The Ca^{2+} microsensor measurements of coral coelenterons are challenging due to the difficulty of constructing the electrodes, which limited the number of profiles we were able to report here. Nevertheless, these are the first documented reports of such profiles and provide valuable insight into the internal chemistry of corals. The calcium concentration inside the mouth in the coelenteron fluid was lower than the calcium concentration in seawater indicating calcium consumption inside the coral (Fig. 2A and C). In both coral species, there was a linear decrease in the Ca^{2+} concentration from the mouth to the coelenteron base, suggesting that the distribution of Ca^{2+} was mainly due to diffusion from the seawater toward the site of calcification at the bottom of the profile and that no uptake of Ca^{2+} occurred elsewhere in the coelenteron (Fig. 2A). Hence, it should be possible to constrain coral calcification rates from the slope of the Ca^{2+} profiles.

Coral calcification rates have traditionally been measured using the alkalinity anomaly method over hours and the buoyant weight technique over several days to weeks (Rodolfo-Metalpa et al., 2010; Schoepf et al., 2017). In principle the Ca^{2+} microsensor method could be used to measure instantaneous calcification rates (on the order of minutes; Tambutté et al. (1996)) through a combination of rapid profiling and modeling of the data. Our initial investigation into this approach shows promise, but further investigation is required to validate the approach and understand the relationship between the rates obtained with more traditional approaches that integrate over larger spatial scales and longer temporal scales such as the buoyant weight and alkalinity anomaly technique.

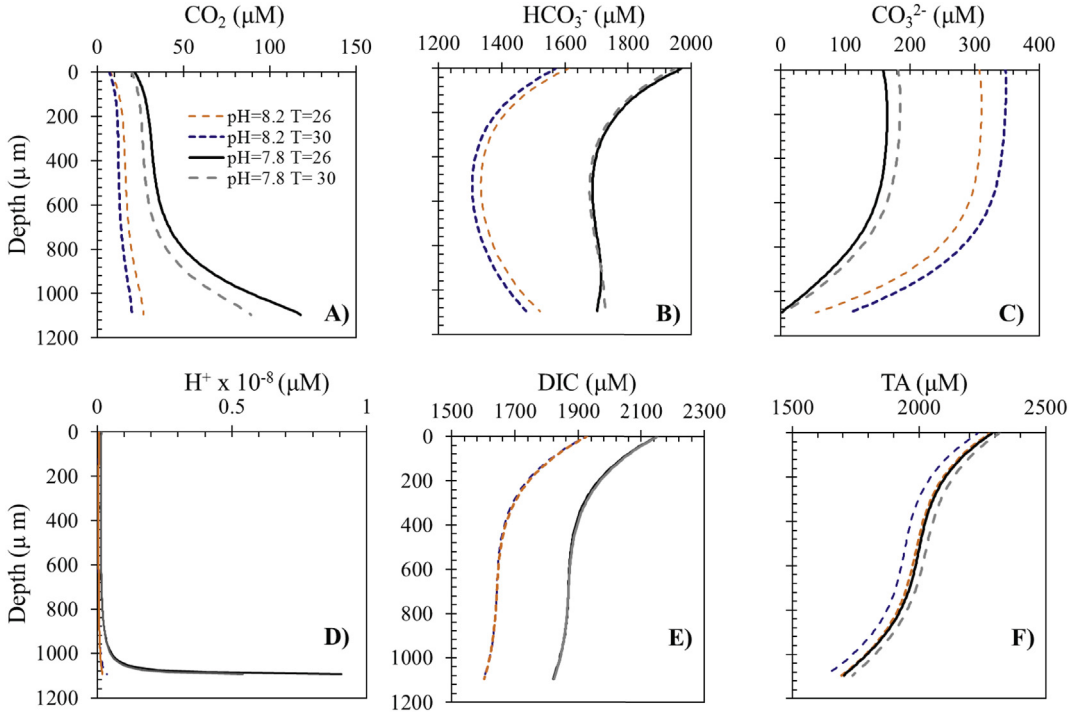

Fig. 3. Simulated profiles of coelenteron A) CO_2, B) HCO_3^-, C) CO_3^{2-}, D) H^+, E) DIC, F) TA concentration at different combinations of seawater pH (7.8 and 8.2) and temperature (26 and 30 °C).

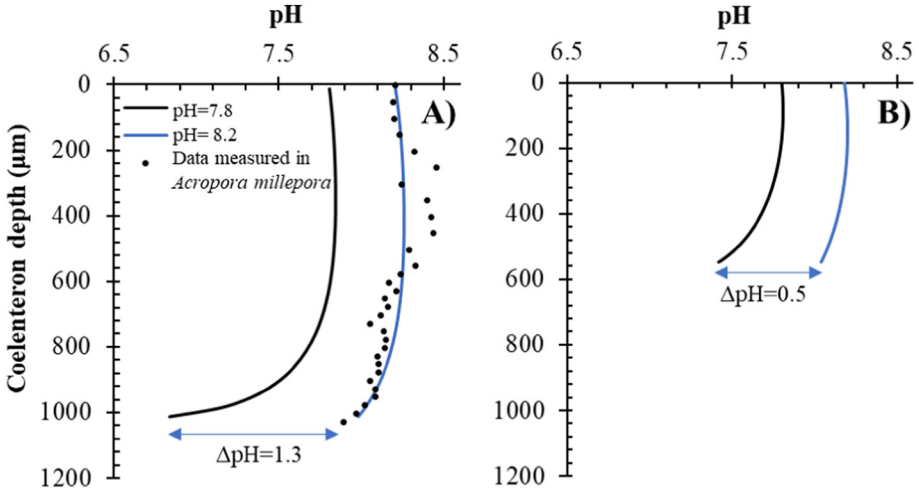

Fig. 4. pH_{NBS} profiles in the coral coelenteron. A) Measured and simulated pH data along coral coelenterons in the scenarios of ambient seawater pH = 7.8 and 8.2 when calcification = 6×10^{-5} μmol cm^{-2} s^{-1} and coelenterons depth = 1100 μm; B) simulated pH data when calcification = 6×10^{-5} μmol cm^{-2} s^{-1} and coelenterons depth = 550 μm. Open circles: the measured data. Lines: simulated data assuming coral metabolism rates and calcification do not change between different scenarios.

4.3. The implications of the H^+ profiles

In contrast to the linear decreases in Ca^{2+} concentration, pH profiles showed a more complex behavior, first increasing in the upper portions of the coral mouth and then decreasing toward the base of the coelenteron in both coral species (Fig. 2B, D). The more complex behavior of pH reflects the multiple processes, including photosynthesis, respiration, and calcification, which affect this variable. Chan et al. (2016) showed that pH increased toward the coral surface due to positive net photosynthesis, and the DBL above the coral surface varied from 50 to 2000 μm depending on water flow (Chan et al., 2016). High pH values in the upper part of the coelenteron are thus a result of CO_2 uptake during photosynthesis (Fig. 2B and D). Between the high pH region in the upper mouth and the lowest pH values at the base of the coelenteron, there is a transition region where pH decreases roughly linearly with depth (Fig. 2B and D). However, since pH is defined as $-\log[H^+]$, one needs to examine the H^+ profile. As H^+ vertical distribution was nonlinear (a concave upward curve), we concluded that H^+ ions were depleted during the diffusion out of the coral coelenterons. At the base of the coelenteron, pH values decreased by ~0.86 ± 0.2 relative to that in seawater (pH = 8.19 ± 0.01) (Fig. 2B and D).

The complex behavior of pH was examined using the reaction-diffusion model and showed that the highest pH in the upper region of the coelenteron was due to photosynthetic CO_2 consumption (Fig. 2B, C and Fig. 3A). The extremely low pH at the base of the coelenteron is attributed to the H^+ pumping from the calcifying fluid (Fig. 2B, C and Fig. 3D). Moving up in the coelenteron from the base, the pH rises rapidly as protons released from the calicoblastic epithelium into the coelenteron are neutralized by the more basic fluid from coral tissue with net photosynthetic activity (i.e., photosynthesis – respiration). In addition to photosynthesis and respiration, organic acids secreted to digest ingested organic matter may also affect the pH in the coelenteron, but this is not accounted for in our model (Agostini et al.,

2011). However, since these corals were not fed prior or during to the microprofile measurements, it is unlikely that digestive acids contributed to the pH of the coelenterons in this study.

The good agreement between modeled and observed pH values in the coelenteron (Fig. 4) is notable given the multiple processes affecting pH. It suggests that the coelenteron can be interpreted using basic aqueous chemistry approaches and conversely that the major processes affecting pH in the coelenteron (metabolic processes, diffusion, and acid-base reactions) are understood. Future studies could employ similar approaches in the coelenteron to investigate ion fluxes, metabolic rates, and the effects of environmental perturbations including temperature stress and ocean acidification on corals.

The H^+ gradient between external seawater and the calcification site has been regarded as an important factor regulating coral calcification (McCulloch et al., 2012; Ries, 2011b). Corals need extra energy to overcome the H^+ gradient and transport proton out of the calcifying fluid as a waste of the calcification process and in exchange for Ca^{2+}. However, our study shows that the gradient between the fluid at the base of coelenteron overlying the calicoblastic epithelium and calcification site is a more appropriate location for estimating the seawater – calcification H^+ gradient. Protons removed from the calcifying fluid appear to be deposited at the base of the coelenteron, lowering the pH in this layer compared to the outside seawater pH. The H^+ ion deposited into the coelenteron may help to convert HCO_3^- to CO_2 that can passively diffuse into the calcifying fluid (McConnaughey and Whelan, 1997), serving to supply inorganic carbon for calcification (Cai et al., 2016). pH at the calcification site was inferred to be 8.3–8.7 using boron isotope techniques (McCulloch et al., 2012) or pH − sensitive dye (Venn et al., 2011; Venn et al., 2009) and up to 10 using a pH microelectrode (Ries, 2011b). Hence, the H^+ concentration at the base of the coelenteron (pH_{NBS} ~7.4) is 10–400 fold higher than in the calcifying fluid. In contrast, the H^+ concentration in external seawater (pH_{NBS} 8.2) is only 2–80 fold higher than the calcifying fluid. Thus, seawater pH may not be as large of a driving factor in calcifying fluid pH levels compared to the biology of the polyps. Our measurements have not been applied to the coral coenosarc. Whether pH in the coelenteric fluid of the coenosarcs is higher than the pH in polyp coelenterons needs further investigation.

The free energy necessary to remove protons from the calcifying fluid has traditionally been estimated using the H^+ gradient between external seawater and the calcification site (Cohen et al., 2009; McCulloch et al., 2012; Ries, 2011a). Using the larger H^+ gradient between the base of the coelenteron (pH_{NBS} 7.4) and the calcifying fluid (pH_{NBS} 8.5) means that a minimum of 6.3 kJ $mol^{-1}H^+$ must be expended to remove protons from the calcifying fluid, which is at least three times larger than the value estimated using the H^+ gradient between the seawater (pH_{NBS} 8.1) and the calcifying fluid (pH_{NBS} 8.5). If a coral exports two H^+ ions from the calcifying fluid per 1 ATP consumed, then the energy required to export these two protons (12.6 kJ mol^{-1}) is approximately a quarter of that produced by ATP hydrolysis (~50 kJ mol^{-1} ATP). This is the minimum energy required to export protons from the calcifying fluid as minimum pH_{NBS} of 8.5 in the calcifying fluid is used for the calculation, yet the realistic energy expenditure on transport need further investigation.

4.4. Numerical simulation of ocean acidification effects based on reaction-diffusion model

In order to study how elevated CO_2 may affect the pH distribution in coral coelenterons, the multiple parameters (CO_2, HCO_3^-, CO_3^{2-}, H^+, DIC and TA) need to be integrated and synthesized with a simulation model, so that the comparison of pH values is possible in responses to elevated CO_2. Here, we were able to explore this issue using the numerical model simulation based on the data range collected with the microelectrodes. Our modeling results of CO_3^{2-} showed a similar distribution pattern to the measured results of Cai et al. (2016) (Fig. 3C), suggesting that our model could provide a reliable prediction of carbonate distribution. Fig. 3A and D showed that CO_2 was elevated at the bottom of coral coelenterons due to high H^+ concentration. The high CO_2 levels in the coral coelenteron are favorable for CO_2 diffusion into the calcifying fluid. In contrast, the DIC and alkalinity decreased with the depth in the coelenteron due to C consumption by calcification at the bottom (Fig. 3E and F).

In addition, our modeling results showed that the low seawater pH expected by the end of this century could affect the vertical distributions of carbonate systems (e.g. CO_2, HCO_3^-, CO_3^{2-} and H^+) more than temperature (Fig. 3). Although ocean warming has exerted great impacts on coral ecosystems (Frieler et al., 2013; Heron et al., 2016), our results showed that temperature increases did not greatly alter carbonate ion diffusion in coral coelenteron if coral metabolism and calcification was not greatly affected by heat stress. Hence, ocean warming likely mainly affected coral biological responses (e.g. coral gene expression (Rocker et al., 2015)) and physiological responses including metabolism and calcification (Grottoli et al., 2014; Jokiel and Coles, 1990) rather than the carbonate ion diffusion.

Keeping photosynthetic and calcification rates constant, our model also predicts that the pH at the base of the coelenteron will decline with decreases in external pH in all scenarios (Fig. 4). The extent of this pH decline is greatly amplified by a deeper coelenteron cavity ($\Delta pH = 1.3$) when compared with a shallower coelenteron ($\Delta pH = 0.5$) due to the reduced transport distance of proton to external seawater in a deeper coelenteron (Fig. 4A and B). Thus, species with deeper polyps should be more sensitive to changes in seawater pCO_2 and pH than shallower polyp corals, and may underlie some of the observed variability in coral responses to OA. Since both *A. millepora* and *T. reniformis* had similar ranges of polyp depths, additional microelectrode profiles of other coral species with different polyp depths are needed to test the model results.

In summary, this work shows that high-resolution chemical profiles through the semi-isolated coelenteron provide valuable information that constrains metabolic fluxes and physiological mechanisms of corals. While Ca^{2+} dynamics within the coelenteron primarily reflect seawater input and consumption by calcification, pH dynamics are more complex due to the tightly coupled processes of photosynthesis, respiration, and calcification. Specifically, our data show that pH firstly increased in the upper part of the coelenteron due to photosynthesis, and then decreased to ~7.5–7.8 at the base of the coelenterons due to dark respiration and proton pumping from the calcification fluid. The H^+-gradient between the base of the coelenteron and the calcifying fluid is 10 times higher than previously estimated and further increases under OA. The energy required to export protons from the calcifying fluid was estimated to be ~3 times higher than previously calculated.

Acknowledgements

We acknowledge the support from CAS program (XDA11020204) to X. Y., NSF EF project numbers 1041070 to W-J.C., 1041124 to A.G., 1040940 to M.W., and 1315944 to B.H. & W-J.C. D.Q, and National Key Technology Support Program (2014BAC01B03) to X. Y. Microelectrode work was accomplished in the Cai laboratory at the University of Georgia before it was moved to the University of Delaware. Yuan ZX and Ding Q were visitors in the Cai laboratory carrying out this work.

References

Agostini, S., et al., 2008. New approach to study the coral symbiotic complex: application to vitamin B 12. In: Proc 11th Int Coral Reef Symp, pp. 917–921.

Agostini, S., et al., 2011. Biological and chemical characteristics of the coral gastric cavity. Coral Reefs 31 (1), 147–156.

Al-Horani, F.A., Al-Moghrabi, S.M., de Beer, D., 2003. Microsensor study of photosynthesis and calcification in the scleractinian coral, Galaxea fascicularis: active internal carbon cycle. J. Exp. Mar. Biol. Ecol. 288 (1), 1–15.

Allison, N., Cohen, I., Finch, A.A., Erez, J., Tudhope, A.W., 2014. Corals concentrate dissolved inorganic carbon to facilitate calcification. Nat. Commun. 5, 5741.

Ammann, D.A.A., 1986. Ion-selective Microelectrodes: Principles, Design and

Application. Springer-Verlag, Berlin.
Anagnostou, E., Huang, K.F., You, C.F., Sikes, E.L. and Sherrell, R.M., 2012. Evaluation of boron isotope ratio as a pH proxy in the deep sea coral *Desmophyllum dianthus*: evidence of physiological pH adjustment. Earth Planet. Sci. Lett., 349–350(0): 251–260.
Cai, W.-J., Zhao, P., Wang, Y., 2000. pH and pCO_2 microelectrode measurements and the diffusive behavior of carbon dioxide species in coastal marine sediments. Mar. Chem. 70 (1–3), 133–148.
Cai, W.-J., Luther III, G., Cornwell, J., Giblin, A., 2010. Carbon cycling and the coupling between proton and Electron transfer reactions in aquatic sediments in Lake Champlain. Aquat. Geochem. 16 (3), 421–446.
Cai, W.-J., et al., 2016. Microelectrode characterization of coral daytime interior pH and carbonate chemistry. Nat. Commun. 7, 11144. http://dx.doi.org/10.1038/ncomms11144.
Chan, N.C.S., Wangpraseurt, D., Kühl, M., Connolly, S.R., 2016. Flow and coral morphology control coral surface pH: implications for the effects of ocean acidification. Front. Mar. Sci. 3.
Cohen, A.L., Mcconnaughey, T.A., 2003. Geochemical perspectives on coral mineralization. Rev. Mineral. Geochem. 54 (1), 151–187.
Cohen, A.L., McCorkle, D.C., de Putron, S., Gaetani, G.A., Rose, K.A., 2009. Morphological and compositional changes in the skeletons of new coral recruits reared in acidified seawater: insights into the biomineralization response to ocean acidification. Geochem. Geophys. Geosyst. 10 (7) (n/a-n/a).
Comeau, S., et al., 2017. Coral calcifying fluid pH is modulated by seawater carbonate chemistry not solely seawater pH. Proc. R. Soc. B Biol. Sci. 284 (1847), 20161669.
de Beer, D., Kühl, M., Stambler, N., Vaki, L., 2000. A microsensor study of light enhanced Ca^{2+} uptake and photosynthesis in the reef-building hermatypic coral *Favia sp.*. MEPS 194, 75–85.
Decarlo, T.M., et al., 2017. Community production modulates coral reef pH and the sensitivity of ecosystem calcification to ocean acidification. J. Geophys. Res. 122 (1), 745–761.
Drake, J.L., et al., 2018. Molecular and geochemical perspectives on the influence of CO2 on calcification in coral cell cultures. Limnol. Oceanogr. 63, 107–121.
Falini, G., Fermani, S., Goffredo, S., 2015. Coral biomineralization: a focus on intra-skeletal organic matrix and calcification. Semin. Cell Dev. Biol. 46, 17–26.
Frieler, K., et al., 2013. Limiting global warming to 2°C is unlikely to save most coral reefs. Nat. Clim. Chang. 3 (2), 165–170.
Furla, P., Galgani, I., Durand, I., Allemand, D., 2000. Sources and mechanisms of inorganic carbon transport for coral calcification and photosynthesis. J. Exp. Biol. 203 (22), 3445–3457.
Galloway, S.B., Work, T.M., Bochsler, V.S., Harley, R.A., Kramarsky-Winters, E., McLaughlin, S.M., Meteyer, C.U., Morado, J.F., Nicholson, J.H., Parnell, P.G., et al., 2006. Coral disease and health workshop: coral histopathology II. National Oceanic and Atmospheric Administration (NOAA), Silver Spring.
Grottoli, A.G., et al., 2014. The cumulative impact of annual coral bleaching can turn some coral species winners into losers. Glob. Chang. Biol. 20 (12), 3823–3833.
Han, C., Cai, W.-J., Wang, Y., Ye, Y., 2014. Calibration and evaluation of a carbonate microsensor for studies of the marine inorganic carbon system. J. Oceanogr. 70 (5), 425–433.
Heron, S.F., Maynard, J.A., Hooidonk, R.V., Eakin, C.M., 2016. Warming trends and bleaching stress of the World's coral reefs 1985–2012. Sci. Rep. 6, 38402.
Hoadley, K.D., et al., 2015. Physiological response to elevated temperature and pCO2 varies across four Pacific coral species: understanding the unique host + symbiont response. Sci. Rep. 5, 18371.
Hohn, S., Merico, A., 2012. Modelling coral polyp calcification in relation to ocean acidification. Biogeosciences 9, 4441–4454.
Holcomb, M., et al., 2014. Coral calcifying fluid pH dictates response to ocean acidification. Sci. Rep. 4 (6188), 1182–1186.
Huang, H., et al., 2014. Positive and negative responses of coral calcification to elevated pCO_2: case studies of two coral species and the implications of their responses. Mar. Ecol. Prog. Ser. 502.
Jokiel, P.L., Coles, S.L., 1990. Response of Hawaiian and other Indo-Pacific reef corals to elevated temperature. Coral Reefs 8 (4), 155–162.
Katz, A., Ben-Yaakov, S., 1980. Diffusion of seawater ions. Part II. The role of activity coefficients and ion pairing. Mar. Chem. 8 (4), 263–280.
Li, Y.H., Gregory, S., 1974. Diffusion of ions in sea water and in deep-sea sediments. Geochim. Cosmochim. Acta 38 (5), 703–714.
Mass, T., et al., 2013. Cloning and characterization of four novel coral acid-rich proteins that precipitate carbonates in vitro. Curr. Biol. 23 (12), 1126–1131.
McConnaughey, T., Whelan, J., 1997. Calcification generates protons for nutrient and bicarbonate uptake. Earth Sci. Rev. 42 (1), 95–117.
McCulloch, M., Falter, J., Trotter, J., Montagna, P., 2012. Coral resilience to ocean acidification and global warming through pH up-regulation. Nat. Clim. Chang. 2 (8), 623–627.
Nakamura, T., Nadaoka, K., Watanabe, A., 2013. A coral polyp model of photosynthesis, respiration and calcification incorporating a transcellular ion transport mechanism. Coral Reefs 1–16.
Orr, J.C., et al., 2005. Anthropogenic ocean acidification over the twenty-first century and its impact on calcifying organisms. Nature 437 (7059), 681–686.
Ries, J., 2011a. Acid ocean cover up. Nat. Clim. Chang. 1 (6), 294–295.
Ries, J.B., 2011b. A physicochemical framework for interpreting the biological calcification response to CO_2-induced ocean acidification. Geochim. Cosmochim. Acta 75, 4053–4064.
Ries, J.B., Cohen, A.L., McCorkle, D.C., 2010. A nonlinear calcification response to CO_2-induced ocean acidification by the coral Oculina arbuscula. Coral Reefs 29 (3), 661–674.
Rocker, M.M., et al., 2015. Expression of calcification and metabolism-related genes in response to elevated pCO2 and temperature in the reef-building coral Acropora millepora. Mar. Genomics 24, 313–318.
Rodolfo-Metalpa, R., Martin, S., Ferrier-Pages, C., Gattuso, J.P., 2010. Response of the temperate coral Cladocora caespitosa to mid- and long-term exposure to pCO(2) and temperature levels projected for the year 2100 AD. Biogeosciences 7 (1), 289–300.
Roy, R.N., et al., 1993. The dissociation constants of carbonic acid in seawater at salinities 5 to 45 and temperatures 0 to 45°C. Mar. Chem. 44, 249–267.
Schoepf, V., et al., 2013. Coral energy reserves and calcification in a high-CO_2 world at two temperatures. PLoS One 8 (10), e75049.
Schoepf, V., et al., 2017. Coral calcification under environmental change: a direct comparison of the alkalinity anomaly and buoyant weight techniques. Coral Reefs 36 (1), 13–25.
Sültemeyer, D., Rinast, K.A., 1996. The CO_2 permeability of the plasma membrane of *Chlamydomonas reinhardtii*: mass-spectrometric ^{18}O-exchange measurements from $^{13}C^{18}O_2$ in suspensions of carbonic anhydrase-loaded plasma-membrane vesicles. Planta 200 (3), 358–368.
Tambutté, É., Allemand, D., Mueller, E., Jaubert, J., 1996. A compartmental approach to the mechanism of calcification in hermatypic corals. J. Exp. Biol. 199 (5), 1029–1041.
Venn, A.A., et al., 2009. Imaging intracellular pH in a reef coral and symbiotic anemone. Proc. Natl. Acad. Sci. U. S. A. 106 (39), 16574–16579.
Venn, A., Tambutté, E., Holcomb, M., Allemand, D., Tambutté, S., 2011. Live tissue imaging shows reef corals elevate pH under their calcifying tissue relative to seawater. PLoS One 6 (5), e20013.
Zeebe, R.E., Wolf-Gladrow, D., 2001. CO_2 in Seawater: Equilibrium, Kinetics, Isotopes. Elsevier, Amsterdam.
Zhao, P., Cai, W.J., 1999. pH polymeric membrane microelectrodes based on neutral carriers and their application in aquatic environments. Anal. Chim. Acta 395 (3), 285–291.